Inorg. Chem. **2003**, *42*, 1673–1680

Synthesis and Structure of [*meso*-Triarylcorrolato]silver(III)

Christian Brückner,*,† Cheri A. Barta,†,‡ Raymond P. Briñas,† and Jeanette A. Krause Bauer§

Department of Chemistry, Unit 3060, University of Connecticut, Storrs, Connecticut 06269-3060, and Department of Chemistry Crystallographic Facility, University of Cincinnati, P.O. Box 210172, Cincinnati, Ohio 45221-0172

Received October 17, 2002

An efficient *meso*-triarylcorrole synthesis is detailed, and the formation and spectroscopic properties of their diamagnetic square-planar d^8 Ag(III) complexes are described. The spectroscopic properties of the [corrolato]-Ag(III) complexes are contrasted with those of the corresponding [porphyrinato]Ag(II) complexes. The oxidation state of the central metal in the corrolato complexes was inferred from their diamagnetic NMR spectra, from X-ray photoelectron spectroscopy measurements, and by single-crystal X-ray diffractometry of the [*meso*-tetra-*p*-tolylcorrolato]-silver(III) complex $TTCAg^{III}$, as its toluene solvate (crystal data for $C_{40}H_{29}N_4Ag\cdot C_7H_8$: monoclinic space group *C*2/*c* with $a = 21.4679(19)$ Å, $b = 20.7606(19)$ Å, $c = 16.0122(11)$ Å, $\beta = 93.700(4)°$, $V = 7121.5(10)$ Å^3, $Z = 8$, $R = 0.0453$, and $R_w = 0.1131$). The conformation of the corrolato ligand in the complex is slightly saddled. The Ag(III) complexes are without precedent in the coordination chemistry of corroles. The Ag(III) complexes underline the ability of *meso*-triarylcorroles to stabilize higher oxidation states as compared to the corresponding *meso*-tetraarylporphyrinato complexes.

Introduction

Corroles are tetrapyrrolic fully conjugated macrocycles containing three methine bridges and one direct pyrrole−pyrrole linkage (Figure 1).[1] Both porphyrins and corroles contain 18 π-electron systems with two or one "cross-conjugated" β,β'-double bonds, respectively. The 18 π-system in the contracted framework of corroles is maintained by change of the oxidation state of one nitrogen. Three pyrrole-type nitrogens and one imine-type nitrogen thus line the central cavity of corroles as compared to two nitrogens of each type in porphyrins. These structural differences are reflected in the altered metal coordination properties of these square-planar tetradentate ligands: the smaller trianionic corrolato ligand has a greater ability to stabilize higher central metal oxidation states than the larger dianionic porphyrinato ligand.[2−9] For instance, the stable oxidation states of manganese and iron in their porphyrinato complexes are +III, while in their corrolato complexes they are +IV.[3,7,8]

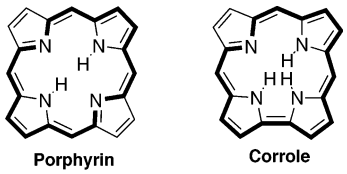

Figure 1. Chromophore structure of porphyrins and corroles, highlighting their 18π-electron systems.

The synthesis of β-octaalkylcorroles is nontrivial.[1] However, the discovery by Gross and co-workers that *meso*-triarylcorroles can be readily synthesized in one step from electron-poor aldehydes and pyrrole rejuvenated the field of corrole coordination chemistry.[9−12] Some of the interest arises

* To whom correspondence should be addressed. Phone: (860) 486-2743. Fax: (860) 486-2981. E-mail: c.bruckner@uconn.edu.
† University of Connecticut.
‡ Current address: Department of Chemistry, University of British Columbia, Vancouver V6T 1Z1, Canada.
§ University of Cincinnati.

(1) Paolesse, R. In *The Porphyrin Handbook*; Kadish, K. M., Smith, K. M., Guilard, R., Eds.; Academic Press: San Diego, 2000; Vol. 2, pp 201−300.
(2) Licoccia, S.; Paolesse, R. *Struct. Bonding (Berlin)* **1995**, *84*, 71−133.
(3) Vogel, E.; Will, S.; Tilling, A. S.; Neumann, L.; Lex, J.; Bill, E.; Trautwein, A. X.; Wieghardt, K. *Angew. Chem., Int. Ed. Engl.* **1994**, *33*, 731−735.
(4) Will, S.; Lex, J.; Vogel, E.; Schmickler, H.; Gisselbrecht, J.-P.; Haubtmann, C.; Bernard, M.; Gross, M. *Angew. Chem., Int. Ed. Engl.* **1997**, *36*, 357−361.
(5) Ghosh, A.; Wondimagegn, T.; Parusel, A. B. J. *J. Am. Chem. Soc.* **2000**, *122*, 5100−5104.
(6) Ghosh, A.; Steene, E. *J. Biol. Inorg. Chem.* **2001**, *6*, 740−751.
(7) Golubkov, G.; Bendix, J.; Gray, H. B.; Mahammed, A.; Goldberg, I.; DiBilio, A. J.; Gross, Z. *Angew. Chem., Int. Ed.* **2001**, *40*, 2132−2134.
(8) Gross, Z. *J. Biol. Inorg. Chem.* **2001**, *6*, 733−738.
(9) Wasbotten, I. H.; Wondimagegn, T.; Ghosh, A. *J. Am. Chem. Soc.* **2002**, *124*, 8104−8116.

10.1021/ic0261171 CCC: $25.00
Published on Web 02/05/2003

from the catalytic activity of *meso*-triarylcorrolato chromium, manganese, and iron complexes in epoxidation, hydroxylation, and cyclopropanation reactions, a reactivity correlated with the ability of the ligand to stabilize high metal oxidation states.[13−18] Since the initial *meso*-triarylcorrole syntheses, we and others reported a number of improved, more general or complementary methodologies.[9,12,19−26]

On the basis of our earlier communication,[23] we detail here an efficient synthesis of *meso*-triphenyl- ($TPCH_3$) and *meso*-tri-*p*-tolylcorrole ($TTCH_3$). Further, we will report the silver complexes of *meso*-triarylcorroles. To the best of our knowledge, no examples of silver corrolato complexes were reported to date.[27] The stable oxidation state of silver in porphyrinato complexes is d^9 Ag(II).[28,29] In contrast, we will demonstrate here using a variety of spectroscopic methods and single-crystal X-ray diffractometry that the stable oxidation state of silver corrolato complexes is +III. The structural determination will also furnish the first structurally characterized corrolato metal complex exhibiting a saddled macrocycle conformation.

Experimental Section

Materials and Instrumentation. All solvents and reagents were used as received. Known 5-phenyldipyrromethane, 5-(4-methylphenyl)dipyrromethane, 5-(4-nitrophenyl)dipyrromethane, and 5-(4-methoxyphenyl)dipyrromethane were prepared as described before.[30,31] 5-(3,5-Dimethoxyphenyl)dipyrromethane was synthesized following a general literature procedure and purified by column chromatography.[30] The analytical thin-layer chromatography (TLC) plates were aluminum backed Silicycle ultrapure silica gel 60, 250 μm; preparative TLC plates (500 μm silica gel on glass) and the flash column silica gel (standard grade, 60 Å, 32−63 μm) used were provided by Sorbent Technologies, Atlanta, GA. The use of a Varian Chroma..Zone flash chromatography system proved to be advantageous for the rapid chromatographic separation of synthetic intermediates and final products. ^{1}H and ^{13}C NMR spectra were recorded on a Bruker DRX400. The NMR spectra are expressed on the δ scale and were referenced to residual solvent peaks. UV−vis spectra were recorded on a Cary 50 spectrophotometer and IR spectra on a Perkin-Elmer Model 834 FT-IR. ESI mass spectra were recorded on a Micromass Quattro II. High-resolution FAB mass spectra were provided by the Mass Spectrometry Facility, Department of Chemistry and Biochemistry, University of Notre Dame (Bill Boggess). Elemental analyses were provided by Numega Resonance Labs Inc., San Diego, CA.

X-ray Photoelectron Spectroscopy. XPS analyses were carried out on a Leybold-Heraeus model 3000 spectrometer upgraded with a SPECS EA10MCD energy analyzer. Samples were prepared by evaporation of a benzene solution of the corroles onto a silicon wafer. Samples did not show any sign of charging as evidenced by the reproducibility of the data and the position of the C 1s and N 1s peaks. The XPS data are summarized in Table 1.

Table 1. XPS Binding Energies (eV) of Free Base Corrole $TTCH_3$ and its Silver Complex $TTCAg^{III}$ in Comparison with Literature Data[a]

	Ag $3d_{3/2}$	Ag $3d_{5/2}$	C 1s	N 1s	ref
$TPPH_2$	*b*	*b*	284.5	399.4 397.3	57
$TTCH_3$	*b*	*b*	284.44[c]	399.59 397.69	this work
$TPPAg^{II}$	373.7	367.6	284.3	398.3	58
$[TPPAg^{III}](ClO_4)$	377.1	371.0	284.2	398.7	58
$TTCAg^{III}$	377.66 (376.83)[d]	371.70 (370.86)[d]	284.70	398.94	this work

[a] For the complete data set of the XPS analyses see Supporting Information. [b] Not applicable. [c] The sp^3 carbon signal expected for the *p*-methyl groups cannot be distinguished from adventitious carbons signals. [d] The shoulders in the Ag $3d_{3/2}$ and $3d_{5/2}$ peak regions (see Figure 4) could be modeled assuming two species with the binding energies listed (for the details of the curve fitting see Supporting Information). The observation of two species is reproducible though their relative ratios varied from sample to sample. We thus assume the origin of the two Ag species to be a crystalline and an amorphous phase formed during the film deposition by evaporation of a dilute benzene solution of the substrates onto the silicon wafer.

X-ray Crystallography.[32] Single crystals of $TTCAg^{III}\cdot C_7H_8$ were obtained by slow evaporation of a toluene solution. A crystal of the approximate dimensions 0.015 × 0.010 × 0.010 mm was mounted on the tip of a loop with paratone-*N* and bathed in a cold stream. The intensity data were collected on a Kappa goniostat (2θ = 5°, others = 0°) with a SMART6000 CCD detector at ChemMatCARS Sector 15 (Advanced Photon Source, Argonne National Laboratory) using synchrotron radiation tuned to the Ag Kα line, λ = 0.559 40 Å. The detector was set at a distance of 5.000 cm from the crystal. For data collection ϕ scan frames were

(10) Gross, Z.; Galili, N.; Simkhovich, L.; Saltsman, I.; Botoshansky, M.; Bläser, D.; Boese, R.; Goldberg, I. *Org. Lett.* **1999**, *1*, 599−602.
(11) Gross, Z.; Galili, N.; Saltsman, I. *Angew. Chem., Int. Ed.* **1999**, *38*, 1427−1429.
(12) Gryko, D. T. *Eur. J. Org. Chem.* **2002**, 1735−1743.
(13) Gross, Z.; Simkhovich, L.; Galili, N. *Chem. Commun.* **1999**, 599−600.
(14) Gross, Z.; Golubkov, G.; Simkhovich, L. *Angew. Chem., Int. Ed.* **2000**, *39*, 4045−4047.
(15) Meier-Callahan, A. E.; Di Bilio, A. J.; Simkhovich, L.; Mahammed, A.; Goldberg, I.; Gray, H. B.; Gross, Z. *Inorg. Chem.* **2001**, *40*, 6788−6793.
(16) Simkhovich, L.; Gross, Z. *Tetrahedron Lett.* **2001**, *42*, 8089−8092.
(17) Bendix, J.; Dmochowski, I. J.; Gray, H. B.; Mahammed, A.; Simkhovich, L.; Gross, Z. *Angew. Chem., Int. Ed.* **2000**, *39*, 4048−4051.
(18) Bendix, J.; Gray, H. B.; Golubkov, G.; Gross, Z. *Chem. Commun.* **2000**, 1957−1958.
(19) Paolesse, R.; Mini, S.; Sagone, F.; Boschi, T.; Jaquinod, L.; Nurco, D. J.; Smith, K. M. *Chem. Commun.* **1999**, 1307−1308.
(20) Ka, J.-W.; Cho, W.-S.; Lee, C.-H. *Tetrahedron Lett.* **2000**, *41*, 8121−8125.
(21) (a) Gryko, D. T. *Chem. Commun.* **2000**, 2243−2244. (b) Gryko, D. T.; Koszarna, B. *Org. Biomol. Chem.* **2003**, *1*, 350−357.
(22) Gryko, D. T.; Jadach, K. *J. Org. Chem.* **2001**, *66*, 4267−4275.
(23) Briñas, R. P.; Brückner, C. *Synlett* **2001**, 442−444.
(24) Asokan, C. V.; Smeets, S.; Dehaen, W. *Tetrahedron Lett.* **2001**, *42*, 4483−4485.
(25) Gryko, D. T.; Piechota, K. E. *J. Porphyrins Phthalocyanines* **2002**, *6*, 81−97.
(26) Guilard, R.; Gryko, D. T.; Canard, G.; Barbe, J.-M.; Koszarna, B.; Brandès, S.; Tasior, M. *Org. Lett.* **2002**, *4*, 4491−4494.
(27) Barta, C. A.; Briñas, R. P.; Brückner, C. In *Abstracts of Papers*, 223rd ACS National Meeting, Orlando, FL, April 7−11, 2002; American Chemical Society: Washington, D.C., 2002; CHED-586.
(28) Kadish, K. M.; Lin, X. Q.; Ding, J. Q.; Wu, Y. T.; Araullo, C. *Inorg. Chem.* **1986**, *25*, 3236−3242.
(29) Scheidt, W. R.; Mondal, J. U.; Eigenbrot, C. W.; Adler, A.; Radonovich, L. J.; Hoard, J. L. *Inorg. Chem.* **1986**, *25*, 795−799.
(30) Boyle, R. W.; Brückner, C.; Posakony, J.; James, B. R.; Dolphin, D. *Org. Synth.* **1999**, *76*, 287−293. (The synthesis of 5-phenyldipyrromethane on 8+*g* batches is detailed. We experienced no problems when scaling the reaction 3-fold.)
(31) Littler, B. J.; Miller, M. A.; Hung, C.-H.; Wagner, R. W.; O'Shea, D. F.; Boyle, P. D.; Lindsey, J. S. *J. Org. Chem.* **1999**, *64*, 1391−1396.
(32) *SMART v5.622 (2001) and SAINT v6.02A (2001) programs*, Bruker AXS, Inc., Madison, WI. SADABS v2.03 (2000) was used for the application of semi-empirical absorption and beam corrections, SHELXTL v6.1 (2000) was used for the structure solution and generation of figures and tables, both by G. M. Sheldrick, University of Göttingen, Germany and Bruker AXS, Inc. Neutral-atom scattering factors were used as stored in the SHELXTL v6.1.

Table 2. Crystal Data and Structure Refinement for TTCAg^{III}·C$_7$H$_8$

empirical formula	$C_{40}H_{29}N_4Ag\cdot C_7H_8$	vol, Å^3	7121.5(10)
fw, g/mol	765.68	Z	8
temp, °C	−100	λ, Å	0.559 40
space group	*C*2/*c* (No. 15)	D_{calcd}, Mg/m^3	1.428
unit cell dimens		μ, cm^{-1}	3.29
a, Å	21.4679(19)	final *R* indices [$I > 2\sigma(I)$][a]	R1 = 0.0453, wR2 = 0.1131
b, Å	20.7606(19)	*R* indices (all data)[a]	R1 = 0.0508, wR2 = 0.1171
c, Å	16.0122(11)		
α, deg	90		
β, deg	93.700(4)		
γ, deg	90		

[a] $R1 = \sum||F_o| - |F_c||/\sum|F_o|$; $wR2 = [\sum w(F_o^2 - F_c^2)^2/\sum w(F_o^2)^2]^{1/2}$; $w^{-1} = [\sigma^2(F_o^2) + (aP)^2 + bP]$ where $P = (F_o^2 + 2F_c^2)/3$ where *a* and *b* are refined quantities.

measured for a duration of 1 s at 0.3° intervals (Θ range, 2.37−22.02°). Limiting indices were as follows: $-28 < h < +28$, $-27 < k < +27$, $-21 < l < +21$. The data frames were processed using the program SAINT. The data were corrected for decay, Lorentz, and polarization effects as well as absorption (maximum and minimum transmissions, 0.9967 and 0.9951) based on the multiscan technique using SADABS.

The structure was solved by a combination of direct methods (SHELXTL v6.1) and the difference Fourier technique and refined by full-matrix least squares on F^2 (40 697 reflections collected, 8422 unique, $R_{int} = 0.0840$). Non-hydrogen atoms were refined with anisotropic displacement parameters. Hydrogen atoms were either located directly or calculated on the basis of geometric criteria and treated with a riding model. A disordered toluene molecule is present. Since a suitable disorder model was not forthcoming, the molecule was simply refined at full occupancy. The refinement converged satisfactorily. Crystal structure and refinement data for TTCAg^{III}·C$_7$H$_8$ are summarized in Table 2.

***meso*-Triphenylcorrole (TPCH$_3$). General Procedure.** Benzaldehyde (**2** with Ar = phenyl, 76 mL, 0.75 mmol) was added to a stirred solution of 5-phenyldipyrromethane (**1** with Ar = phenyl, 1.0 g, 4.5 mmol)[30] in CH_3CN (30 mL) under an atmosphere of N_2. TFA (58 mL, 0.75 mmol) was added, and, after 3 h of stirring at ambient temperature, the reaction was quenched by addition of Et_3N (0.10 mL, 0.75 mmol). DDQ (0.85 g, 3.75 mmol; alternatively chloranil can be used) dissolved in toluene (30 mL) was added. The quickly darkening mixture was stirred overnight. The volume of the mixture was reduced to little less than half by rotary evaporation, and the resulting mixture was separated by column chromatography (silica, 50% petroleum ether 30−60/CH_2Cl_2). The first major dark green fraction was collected and evaporated to dryness. Recrystallization of the residue from ethanol/water afforded 140 mg (35% yield) of TPCH$_3$ as a dark green powdery solid of analytical purity. The procedure was applicable to the reaction of 9 mmol of **2** to yield 1.9 g of TPCH$_3$ (column size 8 × 45 cm). Spectroscopic and analytical data as reported.[33] ^{1}H NMR (400 MHz, $CDCl_3$): δ 8.83 (br s, 4H), 8.50 (br s, 4H), 8.33 (d, $J = 5$ Hz, 4H), 8.15 (d, $J = 5$ Hz, 2H), 7.85−7.70 (m, 9H) (data included for comparison). ^{1}H NMR (400 MHz, $CDCl_3$ - 1.01 equiv of TFA-d_1): δ 8.82 (d, $J = 4.04$, 2H), 8.77 (d, $J = 4.64$ Hz, 2H), 8.49−8.41 (m, 4H), 8.27 (d, $J = 7.34$, 4H), 8.08 (d, $J = 6.16$, 2H), 7.75−7.60 (m, 9H). ^{13}C NMR (100 MHz, $CDCl_3$ - 1.01 equiv of TFA-d_1): δ 142.2, 139.8, 135.0, 134.7, 131.2, 127.9, 127.3−127.1 (overlapping signals), 125.7, 115.7, 109.7.

5,10,15-Tri-*p*-tolylcorrole (TTCH$_3$). TTCH$_3$ was prepared in 17% yield (10 mmol scale) from 5-(*p*-tolyl)dipyrromethane and *p*-tolylaldehyde following the general procedure but using dry CH_2Cl_2 solvent and a reaction time of 1 h at 0 °C. We empirically found that these conditions (solvent and temperature) gave higher yields than the conditions described for TPCH$_3$. Spectroscopic and analytical data are as previously reported.[33] $R_f = 0.77$ (silica gel-$CHCl_3$).

5,10,15-Tris(4-methoxyphenyl)corrole (T(4-MeO)PCH$_3$). T(4-MeO)PCH$_3$ was prepared in 20% yield (2 mmol scale) from 5-(4-methoxyphenyl)dipyrromethane, 4-methoxybenzaldehyde, and pyrrole according to the general procedure. Spectroscopic and analytical data are as previously reported.[9] $R_f = 0.59$ silica gel-$CHCl_3$.

5,10,15-Tris(3,5-dimethoxyphenyl)corrole (T(3,5-MeO)-PCH$_3$). T(3,5-MeO)PCH$_3$ was prepared in 15% yield (1.5 mmol scale) from 5-(3,5-dimethoxyphenyl)dipyrromethane, 3,5-dimethoxybenzaldehyde, and pyrrole according to the general procedure. $R_f = 0.53$ (silica gel-$CHCl_3$). UV-vis (CH_2Cl_2): λ_{max}, nm (log ϵ) 417 (4.75), 527 (sh, 3.68), 575 (3.96), 616 (3.88), 648 (3.84), 721 (sh, 3.42). ^{1}H NMR (400 MHz, $CDCl_3$): δ 8.7 (br s, 4H), 7.4−7.6 (m, 6H), 6.9 (s, 3H), 4.0 (s, 18), −2.1 (br s, 2H). HR-MS (FAB−PEG, MH^+): Calcd for $C_{43}H_{38}N_4O_6$, 707.2870; found: 707.2903.

5,10,15-Tris(4-nitrophenyl)corrole (T(4-NO$_2$)PCH$_3$). T(4-NO$_2$)-PCH$_3$ was prepared in 17% yield (1.5 mmol scale) from 5-(4-nitrophenyl)dipyrromethane, 4-nitrobenzaldehyde, and pyrrole according to the procedure described for TPCH$_3$. $R_f = 0.59$ (silica gel-$CHCl_3$). Spectroscopic and analytical data are as previously reported.[33]

General Silver Insertion Procedure. *meso*-Triarylcorrole (0.1 mmol) was dissolved in pyridine (10 mL), and silver(I) acetate (55 mg, 0.33 mmol) was added. The deep green corrole solution turns, in due course with the metal insertion, a deep dark red. Quantitative silver insertion takes place upon warming of the solution to ∼80 °C (TLC or UV−vis control). Upon completion, the reaction mixture is filtered through a plug of Celite, the solvent is removed on a rotary evaporator, and the residue is subjected to column or preparative thin-layer plate chromatography (silica, 50% petroleum ether 30−60/CH_2Cl_2).

[*meso*-Triphenylcorrolato]silver(III) (TPCAg^{III}). TPCAg^{III} was prepared in 78% yield (1 mmol scale) according to the general procedure. Dark purple microcrystalline crystals were developed by slow evaporation of a toluene solution and dried under high vacuum at 25 °C. $R_f = 0.86$ (silica− toluene/40% petroleum ether). ^{1}H NMR (400 MHz, $CDCl_3$): δ 7.26−7.31 (m, 9H), 8.19 (d, $J = 8$ Hz, 2H), 8.29 (d, $J = 8$ Hz, 4H), 8.67 (d, $J = 4$ Hz, 2H), 8.71 (d, $J = 4$ Hz, 2H), 8.95 (d, $J = 4$ Hz, 2H), 9.03 (d, $J = 4$ Hz, 2H). ^{13}C NMR (100 MHz, acetone-d_6): δ 141.2, 140.3, 137.7, 135.4, 134.6, 134.5, 134.0, 129.4, 127.7, 127.6, 127.5, 127.4, 127.2, 126.7, 125.4, 119.6, 118.3, 117.7. UV−vis (CH_2Cl_2): λ_{max}, nm (log ϵ) 423 (5.11), 499 (sh, 3.66), 523 (sh, 3.87), 544 (sh, 4.03), 561(4.31), 582 (4.52). MS (APCI+, 100% CH_3CN): *m*/*e* 630 (100, M^+), isotope pattern of molecular ion cluster matches composition $C_{37}H_{23}N_4Ag$. HR-MS (FAB−PEG, M^+): Calcd for

(33) Paolesse, R.; Nardis, S.; Sagone, F.; Khoury, R. G. *J. Org. Chem.* **2001**, *66*, 550−556.

$C_{37}H_{23}N_4{}^{107}Ag$, 630.0974; found: 630.1001. Anal. Calcd for $C_{37}H_{23}N_4Ag$ (found): C, 70.38 (70.10); H, 3.67 (3.59); N, 8.87 (5.57).

[*meso*-Tri-*p*-tolylcorrolato]silver(III) (TTCAg^{III}). TTCAg^{III} was prepared in 75% yield (0.5 mmol scale) according to the general procedure. Dark purple needles were extracted by slow evaporation of a toluene solution. R_f = 0.84 (silica− toluene/40% petroleum ether 30−60). ^{1}H NMR (400 MHz, $CDCl_3$): δ 9.16 (d, J = 4, 2H), 8.95 (d, J = 4, 2H), 8.74 (d, J = 4, 2H), 8.71 (d, J = 4, 2H), 8.20 (d, J = 4 Hz, 4H), 8.10 (d, J = 4 Hz, 2H), 7.55−7.64 (m, 6H), 2.68 (overlapping s, 9H). ^{13}C NMR (100 MHz, acetone-d_6): δ 138.64, 138.31, 137.75, 137.64, 137.4, 135.9, 134.8, 134.6, 130.8, 129.6, 128.7, 128.4, 125.6, 119.8, 118.9, 117.9, 113.7, 21.7, 21.5. UV−vis (CH_2Cl_2): λ_{max}, nm (log ϵ) 423 (4.98), 497 (sh), 524 (sh), 545 (sh), 560 (4.15), 586 (4.43) nm. MS (APCI$^+$, 100% CH_3CN): *m*/*e* 672 (100, M$^+$), isotope pattern of molecular ion cluster matches composition $C_{40}H_{29}N_4Ag$. HR-MS (FAB−PEG, M$^+$): Calcd for $C_{40}H_{29}N_4{}^{107}Ag$, 672.1443; found: 672.1437. Anal. Calcd for $C_{40}H_{29}N_4Ag{\cdot}C_7H_8$ (found): C, 73.44 (73.31); H, 5.24 (5.21); N, 7.29 (7.15).

[*meso*-Tris(4-methoxyphenyl)corrolato]silver(III) (T(4-MeO)PCAg^{III}). T(4-MeO)PCAg^{III} was prepared in 80% yield (0.1 mmol scale) according to the general procedure. R_f = 0.81 (silica− 20% petroleum ether 30−60/CH_2Cl_2). ^{1}H NMR (400 MHz, $CDCl_3$): δ 8.97 (d, J = 4.3 Hz, 2H), 8.88 (d, J = 4.6 Hz, 2H), 8.64 (d, J = 4.8 Hz, 2H), 8.61 (d, J = 4.3 Hz, 2H), 8.20 (d, J = 8.4 Hz, 4H), 8.07 (d, J = 8.5 Hz, 2H), 7.36 (d, J = 8.5 Hz, 4H), 7.31 (d, J = 8.5 Hz, 2H), 4.11 (s, 6H), 4.10 (s, 3H). ^{13}C NMR (100 MHz, $CDCl_3$): δ 159.8, 159.5, 138.8, 135.9, 135.7, 135.0, 134.0, 133.1, 131.1, 129.5, 125.5, 119.6, 118.9, 117.7, 113.5, 113.2, 55.8. UV−vis (CH_2Cl_2): λ_{max}, nm (log ϵ) 423 (5.14), 491 (sh, 3.71), 523 (3.97), 547 (sh, 4.14), 559 (4.29), 589 (4.61) nm. HR-MS (FAB−PEG, M$^+$): Calcd for $C_{40}H_{29}N_4O_3{}^{107}Ag$, 720.1291; found: 720.1257.

[*meso*-Tris(3,5-dimethoxyphenyl)corrolato]silver(III) (T(3,5-MeO)PCAg^{III}). T(3,5-MeO)PCAg^{III} was prepared in 60% yield (0.1 mmol scale) according to the general procedure. Dark purple crystals by solvent exchange from CH_2Cl_2 to ethanol. R_f = 0.84 (silica, 20% petroleum ether 30−60/CH_2Cl_2). ^{1}H NMR (400 MHz, $CDCl_3$): δ 9.21 (d, J = 4.4 Hz, 2H), 9.08 (d, J = 4.8 Hz, 2H), 8.86 (d, J = 4.4 Hz, 2H), 8.84 (d, J = 4.8, 2H), 7.50 (d, J = 2.3 Hz, 4H), 7.41 (d, J = 2.3 Hz, 2H), 6.89 (m, 3H), 4.02 (s, 12H), 3.99 (s, 6H). ^{13}C NMR (100 MHz, $CDCl_3$): δ 160.1, 159.8, 143.4, 142.4, 137.8, 135.9, 135.8, 129.7, 125.7, 120.0, 118.3, 118.1, 113.5, 113.2, 100.4, 100.2, 55.9. UV−vis (CH_2Cl_2): λ_{max}, nm (log ϵ) 424 (5.05), 497 (sh), 523 (sh), 562 (4.32), 581 (4.50). HR-MS (FAB−PEG, M$^+$): Calcd for $C_{43}H_{35}N_4O_6{}^{107}Ag$, 810.1608; found: 810.1581.

[*meso*-Tris(4-nitrophenyl)corrolato]silver(III) (T(4-NO$_2$)PCAg^{III}). T(4-NO$_2$)PCAg^{III} was prepared in 60% yield (0.1 mmol scale) according to the general procedure. Dark purple crystals by solvent exchange from CH_2Cl_2 to EtOH. R_f = 0.78 (silica, 20% petroleum ether 30−60/CH_2Cl_2). ^{1}H NMR (400 MHz, DMSO-d_6): δ 9.40 (d, J = 4.5, Hz, 2H), 9.08 (d, J = 4.8 Hz, 2H) 8.87 (d, J = 4.5, 2H), 8.84 (d, J = 4.8 Hz, 2H), 8.75 (d, J = 8.6 Hz, 4H), 8.72 (d, J = 8.6 Hz, 4H), 8.59 (d, J = 8.6 Hz, 2H), 8.49 (d, J = 8.6 Hz, 2H). UV−vis (CH_2Cl_2): λ_{max}, nm (log ϵ) 441 (4.94), 547 (sh, 4.12), 589 (4.56). MS (APCI+, 100% CH_3CN): *m*/*e* 766 (100, MH$^+$), isotope pattern of molecular ion cluster matches composition $C_{37}H_{21}N_7O_6Ag$.

Results and Discussion

Syntheses of *meso*-Triarylcorroles (TPCH$_3$ and TTCH$_3$). *meso*-Triaryltetrapyrranes (such as **3**) can be oxidatively ring-closed to provide, after aromatization of the macrocycle, the corresponding corroles.[20,23−25,33] Such oxidatively induced formations of direct pyrrole−pyrrole linkages have precedents in pyrrole and pyrrolic macrocycle chemistry and constitute the ring-closing step in all recent triarylcorrole syntheses.[34−37] Hence, key to an efficient triarylcorrole synthesis is the formation of a high yield of the corresponding tetrapyrrane (Scheme 1).

Scheme 1 [a]

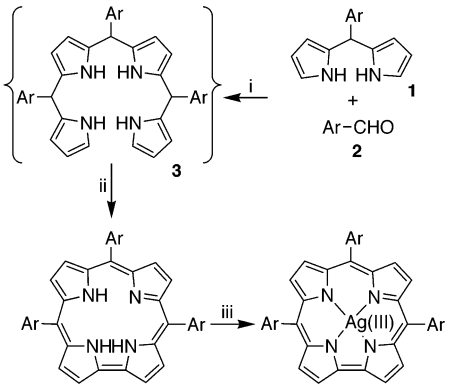

Ar = phenyl: **TPCH$_3$ / TPCAg**
p-tolyl: **TTCH$_3$ / TTCAg**
4-MeO-phenyl: **T(4-MeO)PCH$_3$ / T(4-MeO)PCAg**
4-NO$_2$-phenyl: **T(4-NO$_2$)PCH$_3$ / T(4-NO$_2$)PCAg**
3,5-di-MeO-phenyl: **T(3,5-MeO)PCH$_3$ / T(3,5-MeO)PCAg**

[a] Reaction conditions: (i) TFA, CH_3CN at 25 °C or CH_2Cl_2 at 0 °C. (ii) (a) DDQ or chloranil; (b) column chromatography. (iii) (a) 3.3 equiv of AgAc, pyridine, Δ; (b) column chromatography.

meso-Aryl substituted oligopyrranes (**3**) are compounds of limited stability.[20,36,38] Although they can be isolated and characterized and their oxidation proves unambiguously their role as intermediates in the triarylcorrole formation,[20,36] their isolation is not required for the purpose of an efficient corrole synthesis. Instead, their in situ preparation and immediate oxidation is sufficient.[20,23,24,33] It is, however, important that the intermediate tetrapyrranes be formed without concomitant formation of a porphyrinogen as the subsequent oxidation step would convert this cyclic tetrapyrrolic intermediate to porphyrins.[39] Separation of *meso*-tetraarylporphyrins from their analogous *meso*-triarylcorroles is challenging and impractical when preparing corroles in millimole scales. In fact, the simultaneous formation of porphyrins and corroles during the one-step syntheses of corroles from aldehydes and pyrrole constitutes the major drawback of this otherwise appealing method.[9,19]

Our approach toward the formation of tetrapyrranes, while suppressing the formation of porphyrinogens, is to react a benzaldehyde (**2**) with a large molar excess of dipyrromethane (**1**, 6:1 molar ratio of dippyrane to benzaldehyde) under Lindsey's nonscrambling conditions.[40] The tetrapyrrane

(34) Sessler, J. L.; Seidel, D.; Lynch, V. *J. Am. Chem. Soc.* **1999**, *121*, 11257−11258.
(35) Narayanan, S. J.; Sridevi, B.; Chandrashekar, T. K.; Englich, U.; Ruhlandt-Senge, K. *Org. Lett.* **1999**, *1*, 587−590.
(36) Cho, W.-S.; Lee, C.-H. *Tetrahedron Lett.* **2000**, *41*, 697−701.
(37) Seidel, D.; Lynch, V.; Sessler, J. L. *Angew. Chem., Int. Ed.* **2002**, *41*, 1422−1425.
(38) Brückner, C.; Sternberg, E. D.; Boyle, R. W.; Dolphin, D. *Chem. Commun.* **1997**, 1689−1690.
(39) Dolphin, D. *J. Heterocyclic Chem.* **1970**, *7*, 275−283.

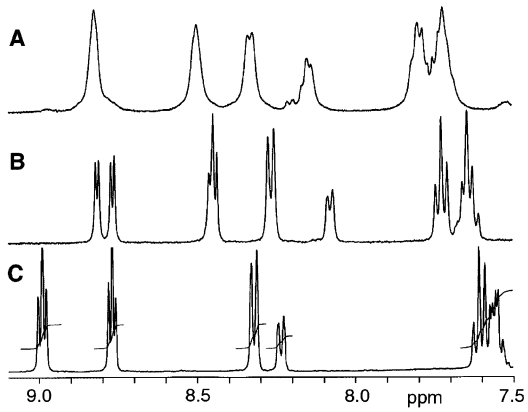

Figure 2. Aromatic region of the ^{1}H NMR ($CDCl_3$, 400 MHz) of (A) $TPCH_3$, (B) $TPCH_3$ in the presence of 1 equiv of TFA-d_1, and (C) $TPCAg^{III}$.

formed is oxidized in situ with DDQ or chloranil. This reaction sequence leads to the formation of none or only traces of the corresponding tetraarylporphyrin (<1%). An increase of the molar excess of the dipyrromethane does not lead to an increase of the corrole yield. The main side products formed are pyrrolic polymers and dipyrrins,[41] polar materials not impeding the chromatographic isolation of the nonpolar triarylcorroles. Using this method, triarylcorroles uncontaminated with porphyrins could be prepared in up to 35% yield (based on limiting reagent **2**, formation of up to 1.9 g of $TPCH_3$ or $TTCH_3$ per run). The apparent waste of the dipyrromethane **1** is balanced by the applicability of the synthesis to relatively large scales and the purity of the resulting corrole and is mitigated by the ease at which dipyrromethanes have become accessible.[30] This methodology adds to a number of largely complementary techniques which were devised in the past 3 years for the synthesis of *meso*-triarylcorroles[9,10,21,22,25,26,36] and *meso*-triarylheterocorroles.[35,36,42]

Free base corroles were described amply before, but a number of new observations are noteworthy. The ^{1}H and ^{13}C NMR spectra of free base corroles is severely broadened (Figure 2A). The X-ray structure of a free base *meso*-triphenylcorrole has proven that it is nonplanar.[10] One of the pyrrolic subunits is tilted so as to reduce the steric crowding of the three NH protons in the central cavity. Thus, the broadened NMR is likely the result of dynamic processes involving the scrambling of the position of the tilted pyrrolic unit and/or swinging of the tilted pyrrolic unit through the center of the macrocycle. Accordingly, rigidified triarylcorroles containing sterically demanding *o*-phenyl substituents display sharper NMR signals.[25] Addition of 1 equiv of TFA protonates the corrole.[11] This evidently also rigidifies the macrocycle, allowing the recording of sharp NMR signals (Figure 2B). Importantly, the NMR allows the conclusion that protonation does not invert one of the pyrrolic units as observed in *meso*-triarylsapphyrin, an expanded corrole.[43] As will be demonstrated below, the NMR and UV−vis spectral characteristics of the protonated corrole serve as reference points for the interpretation of the metalation experiments.

Syntheses [*meso*-Triarylcorrolato]silver(III). Upon warming a solution of *meso*-triarylcorrole ($TPCH_3$ and $TTCH_3$, respectively) with a ~3.3 M excess of silver(I) acetate in pyridine, the initially green solution turns deep red within a few minutes. A fine precipitate of Ag(0) and/or the formation of a silver mirror on the wall of the reaction flask is observed. As gauged by TLC, only one major nonpolar product is formed (R_f = 0.86 (toluene/40% petroleum ether)). Evaporation of the solvent followed by column chromatographic separation of the main product produces a deep purple microcrystalline powder in excellent yields (~80%). The products are air-, light- and water-stable and dissolve in a wide variety of solvents.

The Ag(III) complex forms in a disproportionation reaction: $3Ag^I \rightarrow Ag^{III} + 2Ag^0$. Reduction of the 3.3 M excess of silver(I) acetate reduces the yield of the reaction, and the metal insertion reaction is independent of the presence or absence of oxygen.

Spectroscopic Characterization of $TPCAg^{III}$ and $TTCAg^{III}$. The IR of the complexes provided no indication for the presence of an NH bond. HR-FAB mass spectrometry determined the *m*/*z* composition of the singly charged species to correspond to $C_{37}H_{23}N_4Ag$ and $C_{40}H_{29}N_4Ag$, respectively, the expected composition for the Ag^{III} corrolato complexes. The compounds are, as judged by their nonbroadened NMR spectra, diamagnetic (Figure 2C). The NMR spectra of the silver complexes largely resemble those of the protonated free base corrole (Figure 2B), suggesting that the central metal is coordinated in an N_4 fashion, while the general low-field shift of the β-proton signals in the metal complex indicates a larger degree of planarity as compared to the protonated species. An expansion of the β-region of the ^{1}H NMR spectrum of select Ag^{III} corrolato complexes allowed the identification of the ^4J coupling constant of 0.8 Hz for the coupling of the β-protons with the $^{107/109}$Ag nuclei (I = $^1/_2$). We thus formulate the compounds to be square planar d^8 Ag(III) complexes. Though Ag(III) complexes were considered a rarity,[44,45] our findings find a parallel in the Ag(III) complexes of porphyrins accessible by oxidation of Ag(II) porphyrins using chemical or electrochemical oxidation methods.[46−48] Further, the silver complexes of singly and doubly N-confused porphyrins as well as the closely related carbaporphyrins (featuring N_3C and N_2C_2 donor sets) were also assigned +III oxidation states.[49−51]

(40) Rao, P. D.; Littler, B. J.; Geier, G. R., III; Lindsey, J. S. *J. Org. Chem.* **2000**, *65*, 1084−1092.
(41) Brückner, C.; Karunaratne, V.; Rettig, S. J.; Dolphin, D. *Can. J. Chem.* **1996**, *74*, 2182−2193.
(42) Sridevi, B.; Narayanan, S. J.; Chandrashekar, T. K.; Englich, U.; Ruhlandt-Senge, K. *Chem.-Eur. J.* **2000**, *6*, 2554−2563.
(43) Chmielewsky, P. J.; Latos-Grazynski, L.; Rachlewicz, K. *Chem.-Eur. J.* **1995**, *1*, 68−73.
(44) Cotton, F. A.; Wilkinson, G.; Murillo, C. A.; Bochmann, M. *Advanced Inorganic Chemistry*; 6th ed.; John Wiley & Sons: New York, 1999.
(45) Abedini, M.; Farnia, M.; Kahani, A. *J. Coord. Chem.* **2000**, *50*, 39−42.
(46) Antipas, A.; Dolphin, D.; Gouterman, M.; Johnson, E. C. *J. Am. Chem. Soc.* **1978**, *100*, 7705−7709.
(47) Kadish, K. M.; Lin, X. Q.; Ding, J. Q.; Wu, Y. T.; Araullo, C. *Inorg. Chem.* **1986**, *25*, 3236−3242.
(48) Milgrom, L. R.; Jones, C. C. *J. Chem. Soc., Chem. Commun.* **1988**, 576−578.

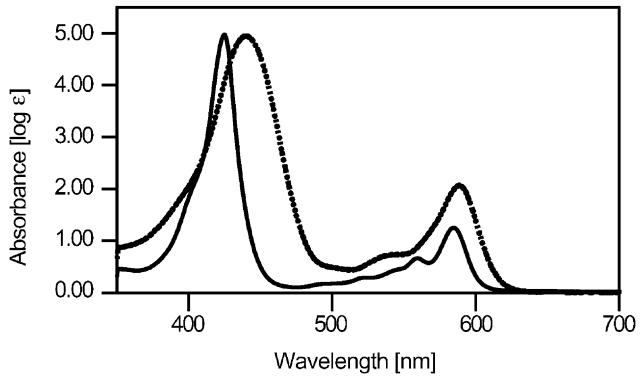

Figure 3. UV−vis spectra ($CDCl_3$) of (−) TTCAg and (--) T(4-NO_2)-$TCAg^{III}$.

UV−Vis Spectral Characterization. The UV−vis spectra of the silver complexes TTCAg and T(4-NO_2)TCAg are shown in Figure 3. The general features of the spectra follow expectations for metallocorroles. The $\lambda_{max} = 586$ nm for the spectrum of TTCAg is significantly blue-shifted compared to the closed d-shell complex [*meso*-tetra(pentafluorophenyl)-corrolato]aluminum(III) ($\lambda_{max} = 620$ nm).[52] Silver(III) corrolato complexes therefore display, using the spectral classification of metalloporphyrins, a typical *hypso* spectrum.[53] Comparing the spectra for TTCAg and the *p*-nitro substituted derivative T(4-NO_2)TCAg, a remarkable influence of the *p*-phenyl substituents on the spectra of the silver(III) corrolato complexes is observed. Ghosh and co-workers recently observed a similar effect in the electronic spectra of *meso*-triarylcorrolato $Fe^{IV}Cl$, $Fe^{IV}OFe^{IV}$, $Mn^{IV}Cl$, and Cu(III) complexes.[9,54] It was interpreted as an indication for a significant ligand-to-metal charge-transfer character of certain transitions in the Soret region of the spectrum and was found to be specific to high-oxidation-state corrolato complexes.[9,46] The silver(III) corrolato complexes follow this observation but to a different extent. While the Soret band in the corrolato Cu(III) complexes shifted bathochromically going from *p*-H (410 nm), to *p*-CH_3 (+8 nm), to *p*-OCH_3 (+23 nm) and shifted hypsochromically upon substitution with electron-withdrawing substituents (*p*-CF_3, −3 nm; C_6F_5−, −4 nm), we observe the Soret for the Ag(III) complexes with *p*-H, *p*-CH_3, *p*-OCH_3 (423 nm), and 3,5-di-OCH_3 (+1 nm) to be almost invariable, whereas the *p*-NO_2 substituted derivative exhibits a bathochromic shift of 17 nm in conjunction with a significantly broadened spectrum.

Parallel to [porphyrinato]Ag^{II} and -Ag^{III} complexes,[46] $TTCAg^{III}$ is nonfluorescent (at 25 °C, CH_2Cl_2). In the porphyrinato complexes, this property was correlated with the existence of low-lying ligand-to-metal charge-transfer bands ($a_{1u}(\pi)$, $a_{2u}(\pi) \rightarrow d_{x^2-y^2}$).[46] Supporting this, the near-IR spectra of the Ag(III) complexes show broad features in the region from 650 to 850 nm, not unlike those observed in the [porphyrinato]Ag^{II} complexes.[46]

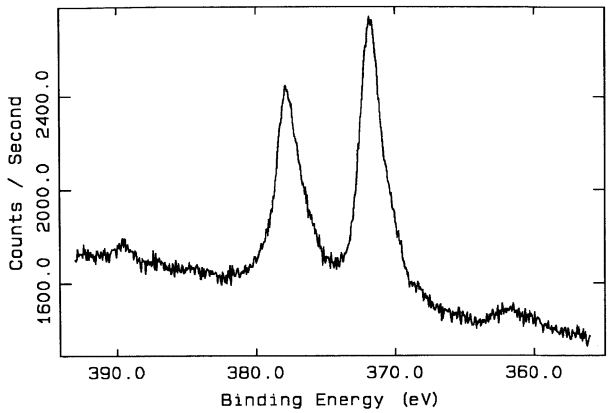

Figure 4. XPS signals in the Ag $3d_{3/2}$ and $3d_{5/2}$ peak region for $TTCAg^{III}$ evaporated onto a silicon wafer. For a tabulation of the data see Table 1.

Demetalation Reaction. The corrolato Ag(III) complexes slowly demetalate in $CHCl_3$ from which traces of acid were not removed, presumably via a reductive mechanism. Hence, treatment of a $CHCl_3$ or CH_2Cl_2 solution of $TPCAg^{III}$ or $TTCAg^{III}$ with concentrated aqueous HCl in a biphasic system leads within minutes to complete demetalation (TLC control) of the silver complex and precipitation of silver(I) chloride. Parallels to the electrochemical reductive or acid-induced demetalations of $TPPAg^{II}$ are clearly evident.[55,56] As far as we are aware, this constitutes the first reversible metalation/demetalation procedure of metallocorroles. Remarkably, treatment of the silver corrolato complexes with gaseous H_2S under neutral conditions does not lead to demetalation. The use of HI leads to the formation of free base and β-iodinated products. The ease of the iodination reaction mirrors the facile exhaustive β-bromination of corroles.[9,33]

X-ray Photoelectron Spectroscopy Study of $TTCH_3$ and $TTCAg^{III}$. XPS has been shown to be an appropriate tool for probing the charge distribution indicative of formal oxidation states in structurally homogeneous systems. Table 1 tabulates the results of an XPS study of the free base corrole $TTCH_3$ and its silver complex $TTCAg^{III}$ in comparison to literature data reported for *meso*-tetraphenylporphyrin $TPPH_2$ and its Ag(II) ($TPPAg^{II}$) and Ag(III) ([$TPPAg^{III}$]-(ClO_4)) complexes.[57,58] The C 1s and N 1s binding energies measured for $TTCH_3$ are equivalent to those found in $TPPH_2$, reflecting the similarity of their carbon sp^2 frameworks containing pyrrole- (sp^3) and imine- (sp^2) type nitrogens (albeit their relative atom-type ratios are different). The Ag $3d_{3/2}$ and $3d_{5/2}$ binding energies (Figure 4) match very well

(49) Furuta, H.; Ogawa, T.; Uwatoko, Y.; Araki, K. *Inorg. Chem.* **1999**, *38*, 2676−2682.
(50) Furuta, H.; Maeda, H.; Osuka, A. *J. Am. Chem. Soc.* **2000**, *122*, 803−807.
(51) (a) Muckey, M. A.; Lash, T. D. *Abstracts of Papers*, 221st ACS National Meeting of the American Chemical Society, San Diego, CA, April 1−5, 2001; American Chemical Society: Washington, D.C., 2001; ORGN-715. (b) Muckey, M. A.; Szczepura, L. F.; Ferrence, G. M.; Lash, T. D. *Inorg. Chem.* **2002**, *41*, 4840−4842.
(52) Mahammed, A.; Gross, Z. *J. Inorg. Biochem.* **2002**, *88*, 305−309.
(53) Gouterman, M. In *The Porphyrins*; Dolphin, D., Ed.; Academic Press: New York, 1978; Vol. III, pp 1−165.
(54) Steene, E.; Wondimagegn, T.; Ghosh, A. *J. Phys. Chem. B* **2001**, *105*, 11406−11413 (Correction/addition: *J. Phys. Chem. B* **2002**, *106*, 5312.
(55) Giraudeau, A.; Louati, A.; Callot, H. J.; Gross, M. *Inorg. Chem.* **1981**, *20*, 769−772.
(56) Krishnamurthy, M. *Inorg. Chem.* **1978**, *17*, 2242−2245.
(57) Karweik, D. H.; Winograd, N. *Inorg. Chem.* **1976**, *15*, 2336−2342.
(58) Karweik, D.; Winograd, N.; Davis, D. G.; Kadish, K. M. *J. Am. Chem. Soc.* **1974**, *96*, 591−592.

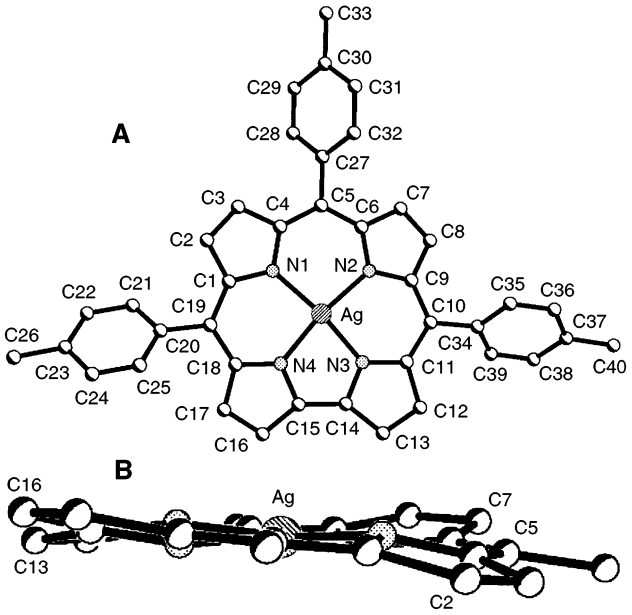

Figure 5. Molecular structure (H-atoms and solvent omitted for clarity; thermal ellipsoids at 50% probability) of TTCAg^{III}·C$_7$H$_8$: (A) top view, with atom labeling; (B) side view along axis of twist (H-atoms and all atoms of the *meso*-*p*-tolyl groups save for the *ipso*-carbons removed for clarity). Select bond distances (Å): Ag−N1, 1.966(2); Ag−N2, 1.955(2); Ag−N3, 1.952(2); Ag−N4, 1.944(2). Angles (deg): N2−Ag−N1, 96.87(9); N4−Ag−N1, 91.82(9); N3−Ag−N2, 91.35(9); N4−Ag−N3, 80.76(9); N3−Ag−N1, 169.76(9); N4−Ag−N2, 169.14(9). Deviation from planarity, root mean square of $C_{23}N_4$ plane: 0.186 Å.

with those previously measured for the Ag(III) salt [TPPAg^{III}]-(ClO_4) and are significantly shifted toward higher binding energies as compared to the energies measured for the Ag-(II) complex TPPAg^{II}, further supporting the presence of a genuine Ag(III) complex. As expected, 3-fold deprotonation and metalation renders all four nitrogens XPS equivalent, supporting the square planar in-plane coordination expected for a d^8 metal ion.

Single-Crystal X-ray Structure Analysis of TTCAg^{III}·C$_7$H$_8$. Proof for the constitution of the Ag(III) complex TTCAg^{III}, as its toluene solvate, was provided by single crystal X-ray crystallography. As only exceedingly fine needles (0.01 × 0.01 × 0.02 mm) could be grown by slow evaporation of a toluene solution of TTCAg^{III}, their crystallographic study was performed at a synchroton beam line at the Advanced Photon Source, Argonne National Laboratory. Crystal data are tabulated in Table 2. A top and side view of the structure is shown in Figure 5; the crystal packing diagram is provided in Figure 6.

The general molecular structure of TTCAg^{III}·C$_7$H$_8$ is as expected for a *meso*-triaryl substituted corrolato complex of a d^8 metal (Figure 5A). The absence of any counterion in conjunction with the absence of any discernible NH protons further confirm the +III oxidation state of the central metal. The central metal is coordinated in a square-planar fashion by the four central nitrogens of the ligand, but the deviations from an ideal square-planar coordination sphere are considerable. The small N3−Ag−N4 bond angle (80.76(9)°) originates in the smaller bite angle of the two nitrogens enforced by the direct pyrrole−pyrrole linkage and is a general characteristic of metallocorroles.[4,15,18,59]

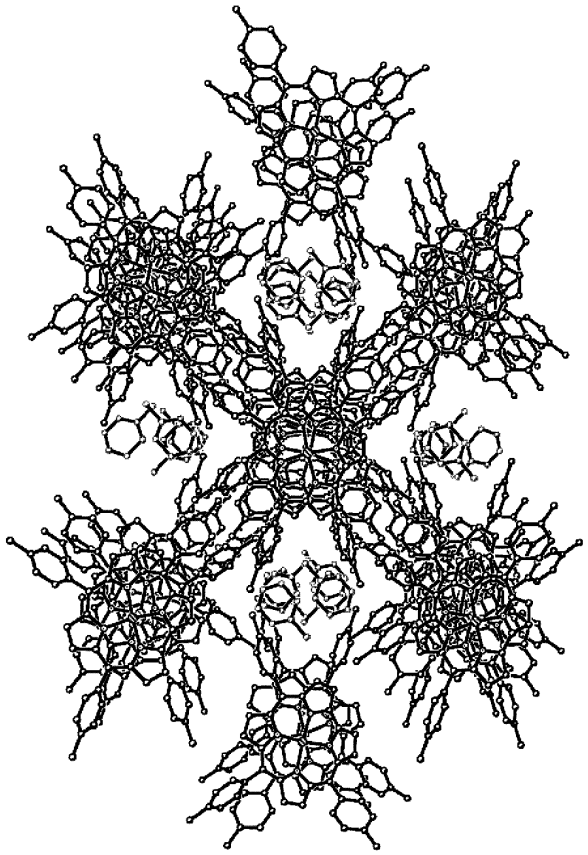

Figure 6. Crystal packing of TTCAg^{III}·C$_7$H$_8$, shown along the crystallographic *a* axis.

The Ag−N bond distances measured vary from 1.966(2) Å (for Ag−N1) to 1.944(2) Å (for Ag−N4). In comparison, the Ag−N bond distances in the planar Ag(II) complex TPPAg^{II} are 2.082(3) and 2.101(3) Å.[29] Interestingly, the Ag−N bond distances measured for the near-planar Ag(III) complexes of carbaporphyrins are similarly long as in the Ag(II) porphyrin complex, namely, 2.03(2)−2.08(2),[49] 2.047(7)−2.064(5),[50] and 2.038(4) − 2.084(4) Å,[51] respectively. Thus, the Ag−N bond distances in these porphyrinic macrocycles are less a reflection of the oxidation state of the central metal but a reflection of the cavity size of the relatively rigid macrocycles. This further allows the conclusion that the origin of the capability of carbaporphyrins and corroles to stabilize high oxidation states of the central metal has a strong electrostatic component. Both ligands are trianionic as compared to the dianionic porphyrins. The better s-donor capabilities of the carbaporphyrins are evidently making up for the smaller size of the corroles. Porphyrins as well as corroles are equally "noninnocent" ligands capable of donating π-density into the metal centers.[5,6]

The corrole chromophore in TTCAg^{III}·C$_7$H$_8$ exhibits a slightly saddled conformation (i.e. the pyrrole rings are alternately tilted above/below the mean plane of the corrole). A twist axis bisects the C14−C15 bond and passes through the central metal and the C5 *meso*-position. Analogous to the effects of any saddling or ruffling in porphyrins, the metal

(59) Simkhovich, L.; Galili, N.; Saltsman, I.; Goldberg, I.; Gross, Z. *Inorg. Chem.* **2000**, *39*, 2704−2705.

is essentially not displaced from the mean plane of the nitrogen donors (only 0.003 Å out of the N1−N4 plane). Hence, the short Ag−N bond distances observed in $TTCAg^{III}\cdot C_7H_8$ are the result of the smaller corrole cavity size, amplified by the distortion of the macrocycle from planarity (Figure 5B), though it is not clear whether this distortion is caused by crystal packing effects or whether it is, in analogy to the conformation of many porphyrin complexes of the (small) Ni(II) ion,[60−62] metal-induced.

This is the first time that a saddled conformation was observed for a metallocorrole, although Ghosh and coworkers most recently calculated the conformation of [*meso*-tri(pentafluorophenyl)corrolato]copper(III) to be saddled.[9] The calculated bond distances for the C−C and C−N bonds in the Cu(III) complex vary, however, from those observed in the saddled Ag(III) complex.

Figure 6 shows the packing diagram for $TTCAg^{III}\cdot C_7H_8$. The corrolato complexes pack in square grid sheets. The sheets are stacked resulting in Ag−Ag separations of 4.31 and 4.04 Å. The square channels between the corrolato stacks are filled with solvate, also forming stacked columns. The observed arrangement is not unlike that found in the crystal structure of a number of *meso*-tetraphenylporphyrin derivatives.[63]

Conclusions

In conclusion, *meso*-triarylcorroles form stable Ag(III) complexes. These complexes underline once again the special ability of corroles to induce the stabilization of higher oxidation states as compared to the corresponding porphyrins. As more Ag(III) complexes of tetrapyrrolic and related ligands become known, this oxidation state for silver cannot be regarded as an exception anymore. In fact, the Ag(III) complexes underline the classic principle of coordination chemistry that the ligand environment largely determines the stable oxidation state of a coordinated metal. The nonplanar conformation of $TTCAg^{III}$ indicates that the coordination chemistry and physical properties of corroles could be modulated by similar conformational effects as porphyrins.[64] Further interesting coordination chemistry of metallocorroles containing metals in unusually high oxidation states can be expected soon, particularly given the ease at which free base *meso*-triarylcorroles have become synthetically accessible or considering their commercial availability.[65]

Acknowledgment. The work was supported with funds provided by the University of Connecticut (UConn) Research Foundation and the donors of the Petroleum Research Fund (PRF), administered by the American Chemical Society. C.A.B. thanks the National Science Foundation for an NSF-REU summer research stipend. We are indebted to Bill Willis and Steven L. Suib, Department of Chemistry, UConn, for the measurement of the XPS data. We thank Stephen Capetta, Department of Chemistry, UConn, for experimental support. X-ray diffractometry investigations were carried out at ChemMatCARS during commissioning time of the beamline, courtesy of J. Viccaro and the University of Chicago. J.A.K.B. would like to thank D. Cookson and T. Graber for support at the beamline. ChemMatCARS Sector 15 is principally supported by the National Science Foundation/Department of Energy under Grant No. CHE0087817 and by the Illinois Board of Higher Education. The Advanced Photon Source is supported by the U.S. Department of Energy, Basic Energy Sciences, Office of Science, under Contract No. W-31-109-Eng-38.

Supporting Information Available: Details of the XPS analysis of $TTCH_3$ and $TTCAg^{III}$ (PDF) and X-ray crystallographic CIF file for $TTCAg^{III}\cdot C_7H_8$. This material is free of charge via the Internet at http://pubs.acs.org. CIF files are available free of charge via the Internet at http://www.ccdc.cam.ac.uk. Refer to CCDC reference number CCDC-202424.

IC0261171

(60) Brückner, C.; Sternberg, E. D.; MacAlpine, J. K.; Rettig, S. J.; Dolphin, D. *J. Am. Chem. Soc.* **1999**, *121*, 2609−2610.
(61) Jentzen, W.; Simpson, M. C.; Hobbs, J. D.; Song, X.; Ema, T.; Nelson, N. Y.; Medforth, C. J.; Smith, K. M.; Veyrat, M.; Mazzanti, M.; Ramasseul, R.; Marchon, J. C.; Takeuchi, T.; Goddard, W. A.; Shelnutt, J. A. *J. Am. Chem. Soc.* **1995**, *117*, 11085−11097.
(62) Kozlowski, P. M.; Rush, T. S., III; Jarzecki, A. A.; Zgierski, M. Z.; Chase, B.; Piffat, C.; Ye, B.-H.; Li, X.-Y.; Pulay, P.; Spiro, T. *J. Phys. Chem. A* **1999**, *103*, 1357−1366.
(63) Byrn, M. P.; Curtis, C. J.; Hsiou, Y.; Khan, S. I.; Sawin, P. A.; Tendick, S. K.; Terzis, A.; Strouse, C. E. *J. Am. Chem. Soc.* **1993**, *115*, 9480−9497.
(64) Shelnutt, J. A.; Song, X.-Z.; Ma, J.-G.; Jentzen, W.; Medforth, C. J. *Chem. Soc. Rev.* **1998**, *27*, 31−41.
(65) *meso*-Triarylcorroles are commercially available: Strem Chemicals, Inc. (www.strem.com).